SCIENCE CHINA
Earth Sciences

SPECIAL TOPIC: China since the Last Glacial Maximum
•REVIEW•

August 2019 Vol.62 No.8: 1181–1192
https://doi.org/10.1007/s11430-018-9254-8

The East Asian Monsoon since the Last Glacial Maximum: Evidence from geological records in northern China

Shiling YANG[1,2,3,4*], Xinxin DONG[5] & Jule XIAO[1,2,3,4]

[1] *Key Laboratory of Cenozoic Geology and Environment, Institute of Geology and Geophysics, Chinese Academy of Sciences, Beijing 100029, China;*
[2] *Institutions of Earth Science, Chinese Academy of Sciences, Beijing 100029, China;*
[3] *CAS Center for Excellence in Life and Paleoenvironment, Beijing 100044, China;*
[4] *University of Chinese Academy of Sciences, Beijing 100049, China;*
[5] *Bureau of General Affairs, Chinese Academy of Sciences, Beijing 100864, China*

Received February 13, 2018; revised June 28, 2018; accepted July 23, 2018; published online September 11, 2018

Abstract The impact of global warming on the climate of northern China has been investigated intensively, and the behavior of the East Asian monsoon during previous intervals of climatic warming may provide insight into future changes. In this study, we use paleovegetation records from loess and lake sediments in the marginal zone of the East Asian summer monsoon (EASM) to reconstruct the EASM during the interval of warming from the Last Glacial Maximum (LGM) to the Holocene. The results show that during the LGM, desert steppe or dry steppe dominated much of northern China; in addition, the southeastern margin of the deserts east of the Helan Mountains had a distribution similar to that of the present-day, or was located slightly further south, due to the cold and dry climate caused by a strengthened East Asian winter monsoon (EAWM) and weakened EASM. During the last deglaciation, with the strengthening of the EASM and concomitant weakening of the EAWM, northern China gradually became humid. However, this trend was interrupted by abrupt cooling during the Heinrich 1 (H1) and Younger Dryas (YD) events. The EASM intensified substantially during the Holocene, and the monsoon rain belt migrated at least 300 km northwestwards, which led to the substantial shrinking of the desert area in the central and eastern part of northern China, and to the large expansion of plants favored by warm and humid conditions. Paleoclimatic records from the marginal zone of the EASM all show that the EASM reached its peak in the mid-Holocene, and past global climatic warming significantly strengthened the EASM, thereby greatly improving the ecological environment in northern China. Thus, northern China is expected to become wetter as global warming continues. Finally, high resolution Holocene vegetation records are sparse compared with the numerous records on the orbital timescale, and there is a need for more studies of Holocene climatic variability on the centennial-to-decadal scale.

Keywords East Asian monsoon, Last Glacial Maximum, Holocene, Paleovegetation, Global warming

Citation: Yang S, Dong X, Xiao J. 2019. The East Asian Monsoon since the Last Glacial Maximum: Evidence from geological records in northern China. Science China Earth Sciences, 62: 1181–1192, https://doi.org/10.1007/s11430-018-9254-8

1. Introduction

The word ‘monsoon’ derives from the Arabic ‘mawsim’, meaning ‘season’. By at least the first century AD, Arabic sailors had noticed that northeasterly winds blowing from India to East Africa prevailed over the Indian Ocean during winter, and that the wind direction reversed during summer. This seasonal monsoon wind reversal was used by them for maritime navigation and trade. In 1686, Edmund Halley, a British astronomer, proposed that the monsoon was driven by the thermal contrast between land and sea (Halley, 1686). This insight had a profound effect on studies of the monsoon

* Corresponding author (email: yangsl@mail.iggcas.ac.cn)

during the subsequent 300 years, and it has become the dominant interpretation of monsoon dynamics. In contrast, however, several recent studies have argued that the monsoon results from a seasonal shift in the Intertropical Convergence Zones (ITCZ) (Gadgil, 2003; Wang, 2009). Irrespective of the dynamics of the monsoon system, its essential features are widely recognized: i.e., a large-scale seasonal wind reversal and the associated wet summers and dry winters.

Asia is the most prominent monsoon region on Earth and the Asian monsoon plays a key role in interhemispheric heat and moisture transport (Webster et al., 1998; Ding, 2004). The monsoon rains sustain over half the world's population, and changes in monsoon intensity can cause major disasters such as floods and droughts in monsoon regions. The Asian monsoon is composed of two primary subsystems: the South Asian (Indian) monsoon and the East Asian monsoon (Figure 1; Chen et al., 1991; Wang et al., 2003). According to Chen et al. (1991), in the south Asian monsoon domain, the summer monsoon is mainly controlled by the tropical climate system, and the influence of the winter monsoon is weak due to the blocking effect of the Tibetan Plateau; and in the East Asian monsoon domain, the summer monsoon is controlled by both the subtropical and tropical climate systems and by cold northerly air masses. The EAWM flows to tropical areas over continents and adjacent oceans east of the Tibetan Plateau, and it even crosses the equator to the southern hemisphere (Chen et al., 1991).

Northern China is located in the marginal zone of the EASM, where the ecological environment is fragile and sensitive to climate change. Since the 1970s, the EASM has weakened, and as a result the monsoon rain belt has migrated southwards, causing frequent droughts in northern China (Wang, 2001; Chase et al., 2003; Ding et al., 2008; Dai et al., 2012). The decreased summer monsoon intensity is attributed by several researchers to anthropogenic global warming (Li et al., 2010); however, others have suggested that it is likely to be caused by increased winter and spring snow and ice cover in the Tibetan Plateau (Ding et al., 2009), and by an ENSO-like mode of sea surface temperature variation (Yang and Lau, 2004). Since the modern ocean-atmosphere system is far out of equilibrium with the elevated CO_2 levels because of the large thermal inertia of the oceans (Levitus et al., 2000; Back et al., 2013), the behavior of the EASM during past warming intervals provides a valuable reference for understanding possible future climate change in East Asia.

The interval from the Last Glacial Maximum (LGM) to the Holocene is the most recent warming period, and offers a useful analog for predicting future hydroclimatic changes (Quade and Broecker, 2009; Yang S L et al., 2015). To date, various proxies have been used in regional monsoon reconstruction during the LGM-Holocene interval (Wang et al., 2010; Shen, 2013; Lu et al., 2013a; Liu et al., 2015; Chen et al., 2016). In this study, to minimize the effect of differences in the responses of different monsoon rainfall proxies, paleovegetation records from lake and loess deposits in northern China were synthesized. Our major aims were to characterize changes in the East Asian monsoon during the interval of climatic warming from the LGM to the Holocene, and to assess the possible future impact of ongoing global warming on the climate of northern China.

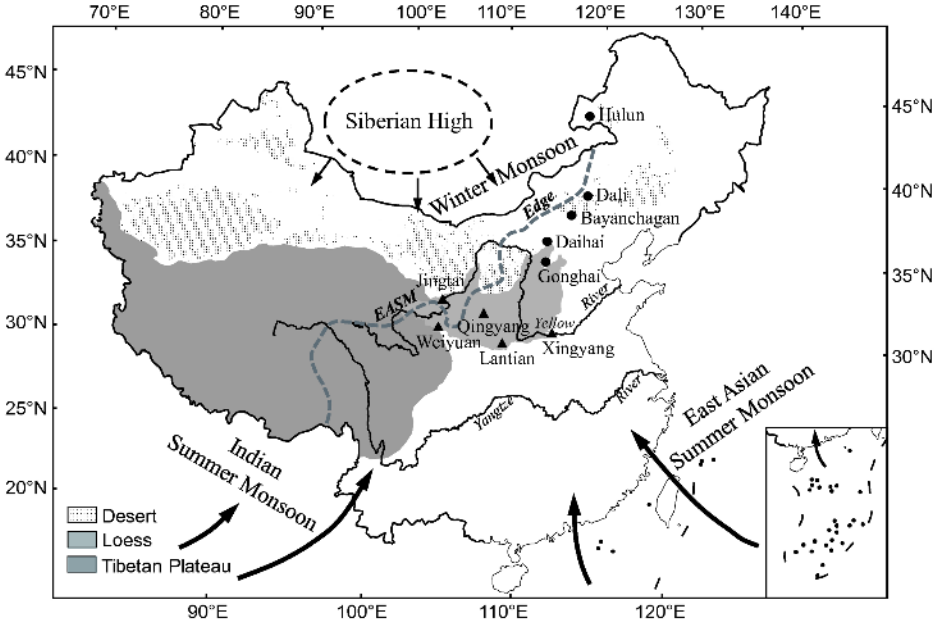

Figure 1 Study sites and location of the northern edge of the East Asian summer monsoon (EASM) (adapted from Xiao et al. (2004)). The dashed line indicates the average position of the northern edge of the EASM during 1979–2000 (Qian et al., 2007).

2. East Asian monsoon variability since the LGM

Earth's climate has undergone a dramatic transition from glacial to interglacial conditions since the LGM, including an increase in atmospheric CO_2 levels from ~180 to ~260 ppmv (Lüthi et al., 2008), an increase of global mean temperature of 5–6°C (Snyder, 2016), and a sea level rise of ~134 m due to large-scale ice melting in the Northern Hemisphere (Lambeck et al., 2014). Against this background, the EASM strengthened and the EAWM weakened from the LGM to the Holocene, and this interval of monsoon variability can be subdivided into three intervals: the LGM, last deglaciation, and Holocene, as described below.

2.1 LGM

During the LGM (26.5–19 ka; Clark et al., 2009), a large ice sheet covered the area of the Scandinavian Peninsula and Barents and Kara Seas; it is known as the 'Barents-Kara' Ice Sheet (Svendsen et al., 2004), with its southern margin at ~52°N. According to model estimates, the center of the ice sheet on the Scandinavian Peninsula was 1800–2100-m thick (Siegert et al., 1999). Meteorological observations have shown that the EAWM system is maintained by the Siberian High (Figure 1), and the cold air developing over the Siberian region comes mainly from the Barents and Kara Seas (Chen et al., 1991). It follows that during the LGM, an intensified Siberian High, caused by the development of the large Barents-Kara Ice Sheet, would have caused a strengthened EAWM and a weakened EASM, thus leading to a southward retreat of the monsoon rain belt.

Northern China experienced a cold and dry climate during the LGM, which is reflected by changes in the extent of deserts and in paleovegetation records. Geological studies (Dong et al., 1996; Sun et al., 2009) have shown that the inland deserts west of the Helan Mountains (Figure 2) may have formed well before the Pleistocene and that there were no significant changes in their extent between glacials and interglacials, while large-scale changes in environment during glacial-interglacial cycles occurred only for the deserts east of the Helan Mountains (Sun et al., 1998; Yang and Ding, 2008; Lu et al., 2013b; Ding and Yang, 2017). At present, the southeastern margins of the deserts east of the Helan Mountains roughly coincide with the mean annual precipitation isohyet of 400 mm, whereas during the LGM the margin of the deserts had a distribution that was generally similar to that of the present-day, or was located slightly further south (Figure 2). The expansion of modern deserts is in contrast to the present interglacial climate, and is thought to be closely related to intensive human activity during the last several thousand years (Zhu, 1998; Sun, 2000; Ding and Yang, 2017).

During the LGM, desert steppe or dry steppe was dominant in most areas of northern China. The vegetation in the northwestern Loess Plateau was characterized by desert steppe, consisting mainly of *Artemisia*, *Echinops*-type, Chenopodiaceae, *Nitraria* and *Ephedra*, and vegetation in the southeastern Loess Plateau was dominated by dry steppe consisting of Poaceae, *Artemisia*, *Taraxacum*-type and *Echinops*-type (Jiang et al., 2013, 2014, 2016; Yang X X et al., 2015). In northeastern China, subalpine meadow prevailed in the Great Khingan Mountains (Wu et al., 2016), and a mosaic of steppe and mixed coniferous and broadleaved forest was dominant around Lake Xingkai (Ji et al., 2015).

In addition to numerous qualitative climatic reconstruc-

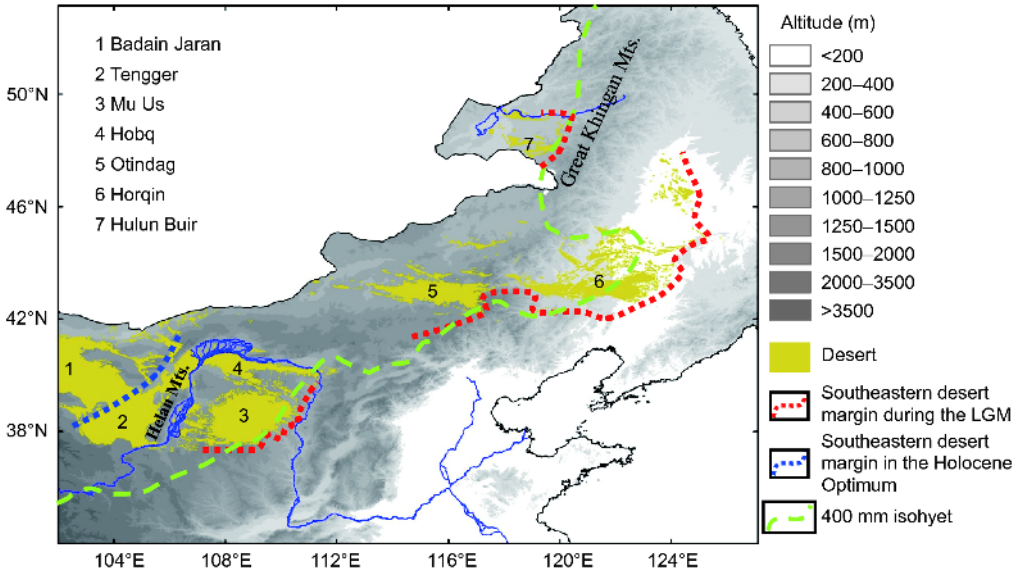

Figure 2 Distribution of the deserts in northern China during the LGM and Holocene Optimum (adapted from Ding and Yang (2017)).

tions, quantitative reconstructions of temperature and precipitation have also been produced for China. Records of magnetic susceptibility and phytoliths from Chinese loess indicate that mean annual precipitation and temperature decreased by ~25–60% (Lu et al., 1994; Heller et al., 1993; Maher et al., 1994; Liu et al., 1995; Lu et al., 2007) and 5–7°C (Lu et al., 2007; Han et al., 1996), respectively, during the LGM relative to the present-day. Recently, a new proxy, glycerol dialkyl glycerol tetraethers (GDGTs), has been applied to loess deposits for paleotemperature reconstruction, and the results indicate temperatures of 14°C, 22°C and 15.5°C at Mangshan during the LGM, mid-Holocene and late Holocene, respectively (Peterse et al., 2014); and temperatures of 15°C, 23°C and 18°C at Lantian during the LGM, mid-Holocene and late Holocene, respectively (Gao et al., 2012). However, it is clear that such reconstructed temperatures cannot be interpreted as mean annual temperatures, but rather they reflect the mean temperature during the growth season of the GDGT-producing bacteria (Gao et al., 2012).

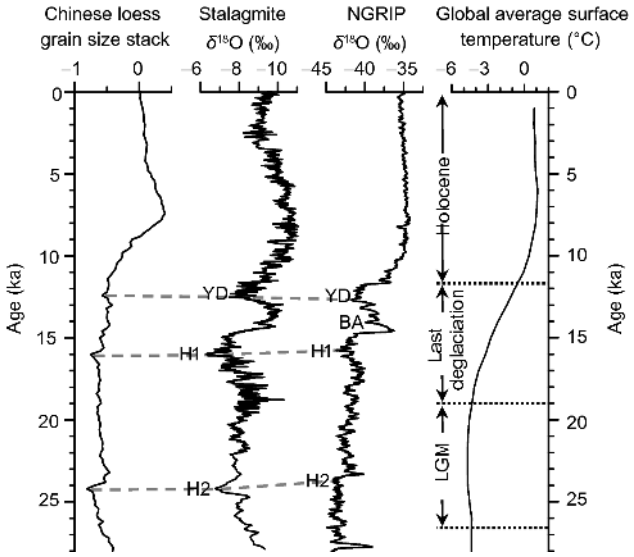

Figure 3 Chinese loess grain-size stack (Yang and Ding, 2014) and the stalagmite δ^{18}O record (Wang et al., 2008) since the LGM from northern China, and their correlation with the NGRIP δ^{18}O record from Greenland (Andersen et al., 2004; Svensson et al., 2008) and global average surface temperature (Snyder, 2016). Lower values of the loess grain-size stack correspond to a coarser grain size, and vice versa.

2.2 Last deglaciation

The last deglaciation (19–11.7 ka) was the interval of global climatic warming from the end of the LGM to the early Holocene (Figure 3; Clark et al., 2012). During the last deglaciation, insolation in the Northern Hemisphere increased and global sea level rose by 80 m, leading to dramatic changes in both terrestrial and marine environments. This cold-warm transition was punctuated by several distinct climatic events, such as the cold Heinrich event 1 (H1, 17.5–16 ka), the warm Bølling-Allerød (BA, 14.7–12.9 ka) and the cold Younger Dryas (YD, 12.9–11.7 ka) (Alley and Clark, 1999) (Figure 3). These millennial-scale climatic events were characterized by abrupt temperature changes of 15–20°C in middle and high latitudes (Severinghaus and Brook, 1999; Liu et al., 2009), comparable to the amplitudes of temperature oscillations during glacial-interglacial cycles.

The H1 event is characterized by coarse-textured loess on the Chinese Loess Plateau (Figure 3; Porter and An, 1995; Ding et al., 1998; Yang and Ding, 2014), reflecting, to a certain extent, the expansion of deserts in northern China, due to the cold and dry climate. Pollen records from the Great Khingan Mountains in northern China also reveal a cold and dry climate during the H1 event, but the humidity was slightly higher than during the LGM (Wu et al., 2016). The last deglaciation was also interrupted by the abrupt cooling event of the Younger Dryas (YD), which may provide insights into possible extreme climatic events under global warming scenarios.

Most studies provide only qualitative estimates of the magnitude of the temperature decrease during the YD event in East Asia. A foraminifera-based quantitative reconstruction from the East China Sea shows that the winter sea surface temperature decreased by 1.5–3.3°C relative to the BA warm period (Wang P X et al., 1996), while the summer sea surface temperature was little changed. A pollen-based quantitative reconstruction from Lake Suigetsu, Japan (Nakagawa et al., 2006), shows that the mean temperature of the coldest month decreased by 4°C and that of the warmest month by 3°C, compared with the BA period. Recently, Wang et al. (2012) identified the occurrence of mirabilite deposition during the YD event in a lake from the Hexi Corridor, northwestern China. Using the relationship between mirabilite deposition and temperature in modern salt lakes, they suggested a drop of 11°C of the mean annual temperature during the YD event relative to today. However, all these quantitative reconstructions need to be verified in future studies.

In northern China, a dry climate prevailed during the YD event. A pollen-based quantitative reconstruction from Lake Gonghai, Shanxi Province indicates an approximate 80-mm decrease in annual precipitation during the YD (Chen et al., 2015). At the same time, in northern China, due to the increased aridity, the loess grain size coarsened (Figure 3; Yang and Ding, 2014), stalagmites recorded high δ^{18}O values (Wang et al., 2008; Ma et al., 2012) or even stopped growing (Cai et al., 2008), and lake levels decreased (Wang et al., 1994). Pollen records from lake sediments in northern China indicate that during the YD, steppe expanded and the extent of woodland decreased, whereas trees such as *Picea*, *Larix* and *Betula*, which are favored by cold climatic conditions, increased (Stebich et al., 2009; Chen et al., 2015; Ji et al.,

2015; Wu et al., 2016).

As early as the 1970s and 1980s, it was proposed that large influxes of glacial meltwater into the North Atlantic reduced northward heat transport in the Atlantic Ocean, thereby causing the cold YD event (Johnson and McClure, 1976; Rooth, 1982). Broecker et al. (1985, 1988) refined this interpretation and suggested a specific physical mechanism (Broecker et al., 1989): The input of large volumes of meltwater into the North Atlantic caused a reduction in surface-water salinity and density and a resultant weakening or shutdown of the Atlantic meridional overturning circulation, thereby leading to the cooling of high northern latitudes and sea ice-expansion. Broecker et al. (1989) further suggested that (1) prior to the YD, the meltwater from Lake Agassiz, which was located around the southwestern margin of the Laurentide Ice Sheet, flowed through the Mississippi River to the Gulf of Mexico; and (2) during the YD event the meltwater was diverted to the northern Atlantic Ocean through the St Lawrence valley. To date, the weakening or shutdown of the thermohaline circulation, due to a major release of meltwater into the North Atlantic, is the preferred mechanism responsible for the YD event. However, other hypotheses have been proposed, including the discharge of Arctic sea-ice (Bradley and England, 2008), the strengthening of the North Atlantic westerlies (Brauer et al., 2008) and the impact of a comet or meteorite (Firestone et al., 2007; Kennett et al., 2009), with the change in meridional overturning circulation potentially being a feedback or response to these events.

According to a recent study of a stalagmite from Kulishu Cave, Beijing, it took ~340 years for the climate to move into the YD, and less than 38 years to move out (Ma et al., 2012). This asymmetry in the structure of the YD event resembles that shown by other stalagmite $\delta^{18}O$ records from the Asian monsoon domain, but it is not observed in paleoclimatic records from Greenland and the North Atlantic (Ma et al., 2012). Due to the short duration of the YD event, as well as the limits of the resolution of paleoclimatic records and uncertainties in climate proxies, several aspects of the YD event are still unclear, including its detailed characteristics, spatial extent, and its effect on the East Asian environment.

2.3 Holocene

Compared with the LGM, the Holocene (11.7 ka to the present) was characterized by a weakened EAWM and a strengthened EASM. As a result, the climatic zones in East Asia migrated northwards and monsoon precipitation increased accordingly, causing dramatic changes in environment such as a shrinking of the area of desert (Figure 2; Sun et al., 1998; Lu et al., 2013b; Ding and Yang, 2017) and an increase in plants favored by warm and humid conditions. However, the spatiotemporal pattern of changes in the East Asian monsoon during the Holocene are debated. Some have suggested a southward time-transgressive pattern of the Holocene Optimum (An et al., 1993; Wu et al., 1994; An et al., 2000), with the wet interval occurring during the early Holocene in northern China, during the mid-Holocene in the middle and lower reaches of the Yangtze River, and during the late Holocene in southern China. In contrast, others have suggested a gradual northward advance of the Holocene Optimum in the East Asian monsoon region (Zhou et al., 2016), with the wet period occurring in the early Holocene in southern China, and in the mid-Holocene in northeastern China.

Numerous monsoon proxy records from a variety of sedimentary records have confirmed that the late Holocene in northern China was characterized by a weakened EASM. However, the timing of the peak in EASM intensity remains controversial. Some have suggested that the early Holocene was a period of maximum summer monsoon precipitation (Chen F H et al., 2001, 2003, 2008; Chen C T A et al., 2003; Zhou et al., 2004), while others have proposed that maximum monsoon precipitation occurred in the mid-Holocene (Xiao et al., 2004, 2008; Wen et al., 2010a, 2010b, 2017; Chen et al., 2015). The reasons for this discrepancy may be largely related to the completeness, continuity and resolution of the geological records, as well as to differences in the climatic significance and sensitivity of the various monsoon proxies employed.

Meteorologists have shown that changes in the intensity of the EASM are essentially reflected by the advance or retreat of the monsoon frontal rainfall belt. It is generally accepted that the more northerly the penetration of the frontal rainfall belt, the greater the intensity of the summer monsoon (Tao and Chen, 1987). The northern edge of the EASM is defined as the northern limit of the monsoon precipitation, which shifts northwards or southwards with interannual fluctuations of the EASM, and thus forms the northern marginal zone of the EASM (Figure 1; Qian et al., 2007; Tang et al., 2010). At present, the northern marginal zone corresponds to the wet-dry transitional area in East Asia which extends in a NE-SW direction. Thus, the environmental system within the marginal zone is very sensitive to monsoon precipitation and paleoclimatic records from lake and loess deposits from the zone are therefore important for constraining the timing of the Holocene Optimum. Next, we summarize the principal features of these records.

2.3.1 Lake records

Pollen records from lakes Daihai (Xiao et al., 2004), Hulun (Wen et al., 2010a), Dali (Wen et al., 2017), Gonghai (Chen et al., 2015) and Bayanchagan (Jiang et al., 2006) (Figure 1), in the marginal zone of the EASM, show that during the early Holocene (11000–8000 yr), steppe consisting of Poaceae, *Artemisia*, Chenopodiaceae and *Ephedra* was dominant in

most areas, indicating a dry climate. However, trees such as *Pinus*, *Betula*, *Ulmus* and *Quercus* were present in several geographically restricted areas (Xiao et al., 2004; Chen et al., 2015). During the mid-Holocene (8000–3000 yr), tree pollen increased, indicating a forest-steppe vegetation, with *Pinus*, *Quercus*, *Betula*, *Ostryopsis* and *Ulmus* dominant in southern areas surrounding lakes Gonghai and Daihai (Xiao et al., 2004; Chen et al., 2015). In northern areas, the vegetation changes can be divided into two periods: (1) During 8000–6000 yr, forest around lakes Dali and Bayanchagan consisted mainly of *Betula*, *Ulmus*, *Quercus* and *Corylus*, and forest around Lake Hulun was dominated by *Betula* and *Corylus*; (2) during 6000–3000 yr, conifers (mainly *Pinus*) increased markedly, while deciduous trees such as *Betula*, *Ulmus* and *Quercus* decreased. During the late Holocene (~3000 yr to the present), steppe vegetation expanded again, and trees in areas around lakes Daihai and Bayanchagan almost disappeared. In contrast, small patches of *Pinus* and *Betula* remained in areas around lakes Gonghai, Dali and Hulun, although the size of these forested areas was much smaller than during the mid-Holocene.

Based on analyses of total organic and inorganic carbon and C/N ratios of a sediment core from Lake Dali, Xiao et al. (2008) inferred a highest lake level during the early Holocene (11500–7600 yr), dramatic fluctuations in lake level during the mid-Holocene (7600–3450 yr), and a general falling trend during the late Holocene (3450 yr to the present). They further proposed that the expansion of the lake during the early Holocene resulted from the input of snow/ice melt from the Great Khingan Mountains, while the rise and fall of the lake level during the mid-Holocene was closely related to changes in monsoonal precipitation.

In the marginal zone of the EASM, the characteristics of quantitative temperature reconstructions vary from site to site. Pollen-based temperature reconstructions from lakes Bayanchagan (Jiang et al., 2006, 2010) and Hulun (Wen et al., 2010b) indicate a warmer early to mid-Holocene than present, while that from Lake Daihai (Xu et al., 2010) shows a cooler early Holocene and a warmer mid-Holocene relative to the present; however, the temperature reconstructions have a comparatively large degree of error and need to be refined. Precipitation reconstructions show similar results (Xu et al., 2010; Wen et al., 2010b; Jiang et al., 2006, 2010; Chen et al., 2015): the mid-Holocene was the wettest interval with an annual precipitation increase of ~20–40% compared to today.

2.3.2 *Loess records*

In the Chinese Loess Plateau, the interval of strongest pedogenic development in the Holocene soil is usually characterized by the finest grain size and highest magnetic susceptibility, reflecting the period of maximum summer monsoon intensity and the minimum area of desert (Yang and Ding, 2008, 2014). Radiocarbon (^{14}C) measurements of soil organic matter from the Jingtai, Weiyuan, Qingyang, Lantian and Xingyang sections (Figure 1) (Yang S L et al., 2015) yielded ages of ~4 ka for the best-developed unit of the Holocene soil. It has been demonstrated that measured ^{14}C ages of soil organic matter are always younger than the actual age of deposition, due to the addition of younger organic matter through rootlet penetration, bioturbation, and percolation of soluble organic substances (Geyh et al., 1983; Wang Y et al., 1996). Therefore, the best developed unit of the Holocene soil should have formed during the mid-Holocene, implying that the mid-Holocene was an interval of maximum monsoon precipitation.

During the Holocene Optimum, *Artemisia* was still dominant in pollen assemblages in the Chinese Loess Plateau. The frequencies of *Echinops*-type, Chenopodiaceae, *Nitraria* and *Ephedra* decreased, while those of Poaceae and tree pollen increased (Jiang et al., 2013, 2014, 2016; Yang X X et al., 2015). From northwest to southeast across the Loess Plateau, *Corylus*, *Quercus*, *Pinus* and Poaceae increased, and *Artemisia* and *Taraxacum*-type decreased. In general, dry steppe prevailed in the northwestern Loess Plateau, while meadow-steppe vegetation dominated in the southeast (Jiang et al., 2014).

Northern Hemisphere insolation increased gradually from the LGM to the early Holocene, peaking at 11 ka, followed by a gradual decrease until the present. However, records from the marginal zone of the EASM all show a monsoon precipitation maximum in the mid-Holocene (~8 ka), lagging the peak in insolation by ~3000 years. This time lag can be attributed to a delay in the northward retreat of the polar front in the North Pacific, due to the persistence of remnant Northern Hemisphere ice sheets, which would have hampered the northward shift of the EASM (Xiao et al., 2008).

2.3.3 *Millennial- to centennial-scale climatic change*

The Holocene climate has traditionally been regarded as relatively stable, and changed gradually in line with variations in Earth orbital parameters and global ice volume. However, Bond et al. (1997) identified 9 cold events, with a quasi-periodicity of 1470 years, in Holocene paleoclimatic records from Greenland and the North Atlantic. These cold events are also documented in stalagmites (Wang et al., 2005) and peats (Hong et al., 2003) in the South Asian monsoon domain, as well as in lake sediments (Chen et al., 2006; Xiao et al., 2009) in the East Asian monsoon area. Bond et al. (2001) further proposed a solar forcing mechanism for the Holocene cold events over the North Atlantic, whereas other studies have suggested several different forcing factors such as ocean circulation (Bianchi and McCave, 1999; Debret et al., 2007), tidal action (Berger and von Rad, 2002), the North Atlantic Oscillation (Giraudeau et al., 2000), and changes in geomagnetic field intensity (St-

Onge et al., 2003).

Recently, a 500-year cyclic climatic change was identified in a 5000-year pollen record from a maar lake in northeastern China (Xu et al., 2015). Tan et al. (2003) reconstructed a 2650-year (665BC–AD1985) warm season temperature record from a stalagmite from Shihua Cave, in Beijing, and identified cycles of 206, 325, 758 and 900 years. These short cycles are usually attributed to solar activity (Tan et al., 2003; Xu et al., 2014), or may be explained by random processes (Turner et al., 2016). Overall, high-resolution studies of Holocene climatic change are sparse and need to be supplemented.

3. Impact of global temperature changes on the EASM in the past and possible impact in the future

3.1 Impact of past global climatic warming on the EASM rain belt

From the LGM to the Holocene Optimum, the EASM rain belt migrated northwards with rising global temperature (Figure 3), leading to a substantial increase in precipitation in East Asia. This shift of the monsoon rain belt is well reflected by changes in the extent of arid regions and vegetation zones. As mentioned earlier, the southeastern desert margins in northern China during the LGM are similar to those of the present (Figure 2; Sun et al., 1998; Yang and Ding, 2008; Lu et al., 2013b; Ding and Yang, 2017). During the Holocene Optimum, the deserts east of the Helan Mountains disappeared entirely. Pollen records suggest that during the Holocene Optimum this region was occupied by *Artemisia* steppe and steppe with spare trees (Jin et al., 2001), which formed a black sand deposit with a relatively high organic matter content. These black sand beds often contain one or more thin, yellow sand layers, as observed in many sections. The ages of these thin sand layers appear to be variable in different deserts, or even within the same desert (Li et al., 1995; Jin et al., 2001; Mason et al., 2009; Yang and Yue, 2011; Lu et al., 2013b), suggesting local-scale sand re-activation that was possibly related to human activity. In addition, an eastward increase in humidity during the Holocene Optimum is identified in the deserts east of the Helan Mountains (Jin et al., 2001). Compared to the LGM, the desert environment retreated northwards by about 300 km, and westwards by over 1000 km, during the Holocene Optimum (Sun et al., 1998; Lu et al., 2013b; Ding and Yang, 2017). Since the development of a desert environment is a result of aridification, an advance of the desert margin can only occur when precipitation is reduced below a critical amount. Consequently, the extent of desert margin migration can be roughly regarded as the migration distance of the EASM rain belt.

Yang S L et al. (2015) measured the $\delta^{13}C$ values of soil organic matter from 21 loess sections (Figure 4) across the Chinese Loess Plateau, and reconstructed the spatial pattern of C_4 biomass for the LGM and Holocene Optimum. The results show that the isolines of C_4 biomass have a northeast-southwest zonal distribution for both intervals, which is consistent with the present-day precipitation pattern: i.e., a northeast-southwest trend for the modern annual isohyets. Therefore, the northeast-southwest zonal distribution pattern of C_4 biomass on the Loess Plateau is a useful analog for the EASM rain belt. Using the plot of 10–20% C_4 biomass as a reference, Yang S L et al. (2015) estimated a minimum 300-km northwestward migration of the monsoon rain belt for the warm Holocene compared with the cold LGM (Figure 4). This estimate is similar to the aforementioned distance of desert margin migration from the LGM to the mid-Holocene.

3.2 Impact of global warming on the climate of northern China

The impacts of global warming are of increasing concern for governments, the scientific community, and societies worldwide (IPCC, 2013). Held and Soden (2006) proposed that, with ongoing global warming, arid regions will become drier, and wet regions will become wetter. The rationale for this conclusion is that rising atmospheric humidity will cause the existing patterns of atmospheric moisture divergence and convergence to become intensified, thus causing effective precipitation to be more negative in dry regions and more positive in wet regions. However, Broecker and Putnam (2013) argue that, as the continents of the Northern Hemisphere warm faster than the Southern Hemisphere oceans, an increase in the interhemispheric temperature contrast will tend to shift the thermal equator (ITCZ) northwards, leading to increased precipitation in monsoonal Asia.

It is noteworthy that the 'southern-flood-northern-drought' climatic pattern in China, observed since the 1970s and caused by a weakening of the EASM intensity, is consistent with the prediction of Held and Soden (2006). However, the geological records of climatic warming during the past 20 ka presented herein demonstrate that increased global temperatures strengthened the EASM and resulted in a concomitant northward advance of the monsoon rain belt. During earlier warm periods, such as Quaternary interglacials (Ding et al., 1999; Yang and Ding, 2008), the Pliocene (Ding et al., 2001; Yang et al., 2018) and the mid-Miocene (Liu et al., 2011; Deng, 2016), northern China was consistently characterized by a wet climate due to increased monsoonal precipitation. Evidently, the geological records strongly support the scenario of Broecker and Putnam (2013). By contrast, the pattern suggested by Held and Soden (2006) would be valid if global warming did not induce shifts in atmospheric circulation patterns, which would indeed

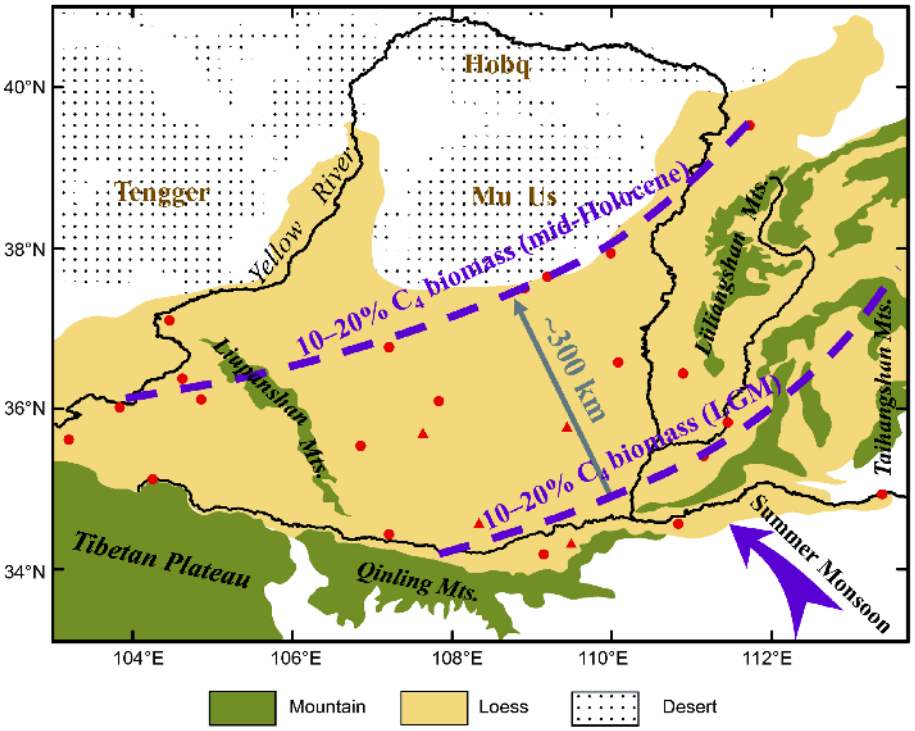

Figure 4 Locations of the East Asian summer monsoon rain belt (purple dashed lines) for the Last Glacial Maximum (LGM) and the mid-Holocene, reconstructed using the 10–20% isolines for C_4 biomass (adapted from Yang S L et al. (2015)).

cause humid regions to become wetter and dry regions to dry further. However, if global warming induced shifts in circulation patterns then an opposing pattern of shifts in precipitation would occur (Allan, 2014). A recent study (Rehfeld and Laepple, 2016) has demonstrated that the relationship between temperature and precipitation is timescale-dependent, i.e., a positive temperature–precipitation relationship in monsoonal Asia on timescales longer than 30–50 years, and a negative temperature–precipitation relationship on time scales shorter than 30 years. We therefore suggest that the drying trend in northern China, which has already lasted for almost nearly half-a-century, will eventually reverse with continued global warming, and indeed a symptom of such a reversal may have already appeared (Ding et al., 2014).

4. Conclusions

In general, there is abundant information available on East Asian monsoon variability for northern China on orbital timescales, including for the interval after the LGM. This information has provided a general picture of Asian monsoon evolution, as well as of the relationship between global temperature and monsoonal precipitation. However, there is a comparative lack of high-resolution Asian monsoon records of sufficient stratigraphic resolution to capture variability on millennial-to-centennial scales, or even shorter, especially of vegetation. In addition, abrupt climatic events and centennial-to-decadal-scale climate variability also merit further investigation, including their expression at different latitudes, including the quantitative reconstruction of climatic parameters, and inter-regional correlations of paleoclimatic records and mechanisms. Such studies are crucial for attaining a better understanding of spatiotemporal changes in the East Asian monsoon and the driving mechanisms, for predicting future climate changes, and for evaluating the ecological effects of global warming. Thus, we suggest that they should be the focus of future geological studies and paleoclimate modelling.

Acknowledgements *We thank Wen R L for providing vegetation data, and Huang X F and Wang Y D for formatting the document. We are grateful to two anonymous reviewers for their constructive comments. This work was supported by the National Key Research and Development Program of China (Grant No. 2017YFA0603403), the Strategic Priority Research Program of the Chinese Academy of Sciences (Grant Nos. XDB26000000 & XDA05120204) and the National Natural Science Foundation of China (Grant Nos. 41672175 & 41725010).*

References

Allan R P. 2014. Dichotomy of drought and deluge. Nat Geosci, 7: 700–701

Alley R B, Clark P U. 1999. The deglaciation of the northern hemisphere: A global perspective. Annu Rev Earth Planet Sci, 27: 149–182

An Z S, Porter S C, Kutzbach J E, Wu X H, Wang S M, Liu X D, Li X Q, Zhou W J. 2000. Asynchronous Holocene optimum of the East Asian monsoon. Quat Sci Rev, 19: 743–762

An Z S, Porter S C, Wu X H, Kutzbach J E, Wang S M, Liu X D, Li X Q, Wang J, Zhou W J, Xiao J Y, Liu J F, Lu J J. 1993. Holocene Optimum of Central and Eastern China and variability of the East Asian monsoon (in Chinese). Chin Sci Bull, 38: 1302–1305

Andersen K K, Azuma N, Barnola J M, Bigler M, Biscaye P, Caillon N, Chappellaz J, Clausen H B, Dahl-Jensen D, Fischer H, Flückiger J, Fritzsche D, Fujii Y, Goto-Azuma K, Grønvold K, Gundestrup N S, Hansson M, Huber C, Hvidberg C S, Johnsen S J, Jonsell U, Jouzel J, Kipfstuhl S, Landais A, Leuenberger M, Lorrain R, Masson-Delmotte V, Miller H, Motoyama H, Narita H, Popp T, Rasmussen S O, Raynaud D, Rothlisberger R, Ruth U, Samyn D, Schwander J, Shoji H, Siggard-Andersen M L, Steffensen J P, Stocker T, Sveinbjörnsdóttir A E, Svensson A, Takata M, Tison J L, Thorsteinsson T, Watanabe O, Wilhelms F, White J W C, White J W C. 2004. High-resolution record of Northern Hemisphere climate extending into the last interglacial period. Nature, 431: 147–151

Back L, Russ K, Liu Z, Inoue K, Zhang J, Otto-Bliesner B. 2013. Global hydrological cycle response to rapid and slow global warming. J Clim, 26: 8781–8786

Berger W H, von Rad U. 2002. Decadal to millennial cyclicity in varves and turbidites from the Arabian Sea: Hypothesis of tidal origin. Glob Planet Change, 34: 313–325

Bianchi G G, McCave I N. 1999. Holocene periodicity in North Atlantic climate and deep-ocean flow south of Iceland. Nature, 397: 515–517

Bond G, Kromer B, Beer J, Muscheler R, Evans M N, Showers W, Hoffmann S, Lotti-Bond R, Hajdas I, Bonani G. 2001. Persistent solar influence on North Atlantic climate during the Holocene. Science, 294: 2130–2136

Bond G, Showers W, Cheseby M, Lotti R, Almasi P, deMenocal P, Priore P, Cullen H, Hajdas I, Bonani G. 1997. A pervasive millennial-scale cycle in North Atlantic Holocene and glacial climates. Science, 278: 1257–1266

Bradley R S, England J H. 2008. The Younger Dryas and the sea of ancient ice. Quat Res, 70: 1–10

Brauer A, Haug G H, Dulski P, Sigman D M, Negendank J F W. 2008. An abrupt wind shift in western Europe at the onset of the Younger Dryas cold period. Nat Geosci, 1: 520–523

Broecker W S, Andree M, Wolfli W, Oeschger H, Bonani G, Kennett J, Peteet D. 1988. The chronology of the last deglaciation: Implications to the cause of the Younger Dryas event. Paleoceanography, 3: 1–19

Broecker W S, Kennett J P, Flower B P, Teller J T, Trumbore S, Bonani G, Wolfli W. 1989. Routing of meltwater from the Laurentide Ice Sheet during the Younger Dryas cold episode. Nature, 341: 318–321

Broecker W S, Peteet D M, Rind D. 1985. Does the ocean-atmosphere system have more than one stable mode of operation? Nature, 315: 21–26

Broecker W S, Putnam A E. 2013. Hydrologic impacts of past shifts of Earth's thermal equator offer insight into those to be produced by fossil fuel CO_2. Proc Natl Acad Sci USA, 110: 16710–16715

Cai B G, Edwards R L, Cheng H, Tan M, Wang X, Liu T S. 2008. A dry episode during the Younger Dryas and centennial-scale weak monsoon events during the early Holocene: A high-resolution stalagmite record from southeast of the Loess Plateau, China. Geophys Res Lett, 35: L02705

Chase T N, Knaff J A, Pielke R A, Kalnay E. 2003. Changes in global monsoon circulations since 1950. Nat Hazards, 29: 229–254

Chen C T A, Lan H C, Lou J Y, Chen Y C. 2003. The dry Holocene Megathermal in Inner Mongolia. Palaeogeogr Palaeoclimatol Palaeoecol, 193: 181–200

Chen F H, Cheng B, Zhao Y, Zhu Y, Madsen D B. 2006. Holocene environmental change inferred from a high-resolution pollen record, Lake Zhuyeze, arid China. Holocene, 16: 675–684

Chen F, Wu W, Holmes J A, Madsen D B, Jin M, Oviatt C G. 2003. A mid-Holocene drought interval as evidenced by lake desiccation in the Alashan Plateau, Inner Mongolia, China. Chin Sci Bull, 48: 1401–1410

Chen F H, Xu Q H, Chen J H, Birks H J, Liu J B, Zhang S R, Jin L Y, An C B, Telford R J, Cao X Y, Wang Z L, Zhang X J, Selvaraj K, Lu H Y, Li Y C, Zheng Z, Wang H P, Zhou A F, Dong G H, Zhang J W, Huang X Z, Bloemendal J, Rao Z G. 2015. East Asian summer monsoon precipitation variability since the last deglaciation. Quat Sci Rev, 27: 351–364

Chen F H, Yu Z C, Yang M L, Ito E, Wang S M, Madsen D B, Huang X Z, Zhao Y, Sato T, Birks H J B, Boomer I, Chen J H, An C B, Wünnemann B. 2008. Holocene moisture evolution in arid central Asia and its out-of-phase relationship with Asian monsoon history. Sci Rep, 5: 11186

Chen F, Zhu Y, Li J, Shi Q, Jin L, Wünemann B. 2001. Abrupt Holocene changes of the Asian monsoon at millennial- and centennial-scales: Evidence from lake sediment document in Minqin Basin, NW China. Chin Sci Bull, 46: 1942–1947

Chen J H, Rao Z G, Liu J B, Huang W, Feng S, Dong G H, Hu Y, Xu Q H, Chen F H. 2016. On the timing of the East Asian summer monsoon maximum during the Holocene—Does the speleothem oxygen isotope record reflect monsoon rainfall variability? Sci China Earth Sci, 59: 2328–2338

Chen L X, Zhu Q G, Luo H B, He J H, Dong M, Feng Z Q. 1991. The East-Asian Monsoon (in Chinese). Beijing: China Meteorol Press. 362

Clark P U, Dyke A S, Shakun J D, Carlson A E, Clark J, Wohlfarth B, Mitrovica J X, Hostetler S W, McCabe A M. 2009. The Last Glacial Maximum. Science, 325: 710–714

Clark P U, Shakun J D, Baker P A, Bartlein P J, Brewer S, Brook E, Carlson A E, Cheng H, Kaufman D S, Liu Z, Marchitto T M, Mix A C, Morrill C, Otto-Bliesner B L, Pahnke K, Russell J M, Whitlock C, Adkins J F, Blois J L, Clark J, Colman S M, Curry W B, Flower B P, He F, Johnson T C, Lynch-Stieglitz J, Markgraf V, McManus J, Mitrovica J X, Moreno P I, Williams J W. 2012. Global climate evolution during the last deglaciation. Proc Natl Acad Sci USA, 109: E1134–E1142

Dai X G, Wang P, Zhang K J. 2012. A decomposition study of moisture transport divergence for inter-decadal change in East Asia summer rainfall during 1958–2001. Chin Phys B, 21: 119201

Debret M, Bout-Roumazeilles V, Grousset F, Desmet M, McManus J F, Massei N, Sebag D, Petit J R, Copard Y, Trentesaux A. 2007. The origin of the 1500-year climate cycles in Holocene North-Atlantic records. Clim Past, 3: 569–575

Deng T. 2016. Records and characteristics of the mammalian faunas of northern China in the Middle Miocene climatic optimum (in Chinese with English abstract). Quat Sci, 36: 810-819

Ding Y H. 2004. Seasonal march of the East-Asian summer monsoon. In: Chang C P, ed. East Asian Monsoon. Singapore: World Scientific Publishing Co. Pte. Ltd. 3–53

Ding Y H, Si D, Sun Y, Liu Y J, Song Y F. 2014. Inter-decadal variations, causes and future projection of the Asian summer Monsoon. Eng Sci, 12: 22–28

Ding Y, Sun Y, Wang Z, Zhu Y, Song Y. 2009. Inter-decadal variation of the summer precipitation in China and its association with decreasing Asian summer monsoon Part II: Possible causes. Int J Climatol, 29: 1926–1944

Ding Y, Wang Z, Sun Y. 2008. Inter-decadal variation of the summer precipitation in East China and its association with decreasing Asian summer monsoon. Part I: Observed evidences. Int J Climatol, 28: 1139–1161

Ding Z L, Rutter N W, Liu T S, Sun J M, Ren J Z, Rokosh D, Xiong S F. 1998. Correlation of Dansgaard-Oeschger cycles between Greenland ice and Chinese loess. Paleoclimates, 2: 281–291

Ding Z L, Xiong S F, Sun J M, Yang S L, Gu Z Y, Liu T S. 1999. Pedostratigraphy and paleomagnetism of a ~7.0 Ma eolian loess-red clay sequence at Lingtai, Loess Plateau, north-central China and the implications for paleomonsoon evolution. Palaeogeogr Palaeoclimatol Palaeoecol, 152: 49–66

Ding Z L, Yang S L. 2017. Plio-Pleistocene changes in the arid and semi-arid regions of northern China on geological time-scales. In: Fu C, Mao H, eds. Aridity Trend in Northern China. Singapore: World Scientific Publishing Co. Pte. Ltd. 5–26

Ding Z L, Yang S L, Sun J M, Liu T S. 2001. Iron geochemistry of loess and red clay deposits in the Chinese Loess Plateau and implications for

long-term Asian monsoon evolution in the last 7.0 Ma. Earth Planet Sci Lett, 185: 99–109
Dong G, Wang G, Chen H, Hasi. 1996. The formation and evolution of deserts in China. In: Geological Society of China, ed. Progress in Geology of China (1993–1996): Papers to 30th IGC. Beijing: China Ocean Press. 1001–1005
Firestone R B, West A, Kennett J P, Becker L, Bunch T E, Revay Z S, Schultz P H, Belgya T, Kennett D J, Erlandson J M, Dickenson O J, Goodyear A C, Harris R S, Howard G A, Kloosterman J B, Lechler P, Mayewski P A, Montgomery J, Poreda R, Darrah T, Hee S S Q, Smith A R, Stich A, Topping W, Wittke J H, Wolbach W S. 2007. Evidence for an extraterrestrial impact 12,900 years ago that contributed to the megafaunal extinctions and the Younger Dryas cooling. Proc Natl Acad Sci USA, 104: 16016–16021
Gadgil S. 2003. The Indian monsoon and its variability. Annu Rev Earth Planet Sci, 31: 429–467
Gao L, Nie J S, Clemens S, Liu W G, Sun J M, Zech R, Huang Y S. 2012. The importance of solar insolation on the temperature variations for the past 110 kyr on the Chinese Loess Plateau. Palaeogeogr Palaeoclimatol Palaeoecol, 317-318: 128–133
Geyh M A, Roeschmann G, Wijmstra T A, Middeldorp A A. 1983. The unreliability of ^{14}C dates obtained from buried sandy Podzols. Radiocarbon, 25: 409–416
Giraudeau J, Cremer M, Manthé S, Labeyrie L, Bond G. 2000. Coccolith evidence for instabilities in surface circulation south of Iceland during Holocene times. Earth Planet Sci Lett, 179: 257–268
Halley E. 1686. An historical account of the trade winds, and monsoons, observable in the seas between and near the tropicks, with an attempt to assign the physical cause of the said winds. Phil Trans, 16: 153–168
Han J M, Lu H Y, Wu N Q, Guo Z T. 1996. The magnetic susceptibility of modern soils in China and its use for paleoclimate reconstruction. Stud Geophys Geod, 40: 262–275
Held I M, Soden B J. 2006. Robust responses of the hydrological cycle to global warming. J Clim, 19: 5686–5699
Heller F, Shen C D, Beer J, Liu X M, Liu T S, Bronger A, Suter M, Bonani G. 1993. Quantitative estimates of pedogenic ferromagnetic mineral formation in Chinese loess and palaeoclimatic implications. Earth Planet Sci Lett, 114: 385–390
Hong Y T, Hong B, Lin Q H, Zhu Y X, Shibata Y, Hirota M, Uchida M, Leng X T, Jiang H B, Xu H, Wang H, Yi L. 2003. Correlation between Indian Ocean summer monsoon and North Atlantic climate during the Holocene. Earth Planet Sci Lett, 211: 371–380
IPCC. Climate Change. 2013. The Physical Science Basis. In: Stocker T F, Qin D, Plattner G K, Tignor M, Allen S K, Boschung J, Nauels A, Xia Y, Bex V, Midgley P M, eds. Working Group I Contribution to the Fifth Assessment Report of the Intergovernmental Panel on Climate Change. Cambridge: Cambridge University Press
Ji M, Shen J, Wu J, Wang Y. 2015. Paleovegetation and paleoclimate evolution of past 27.7 cal ka BP recorded by pollen and charcoal of Lake Xingkai, Northeastern China. In: Kashiwaya K, Shen J, Kim J Y, eds. Earth Surface Processes and Environmental Changes in East Asia: Records from Lake-catchment Systems. Tokyo: Springer. 81–94
Jiang W Y, Chen Y F, Yang X X, Yang S L. 2013. Chinese Loess Plateau vegetation since the Last Glacial Maximum and its implications for vegetation restoration. J Appl Ecol, 50: 440–448
Jiang W Y, Guiot J, Chu G Q, Wu H B, Yuan B Y, Hatté C, Guo Z T. 2010. An improved methodology of the modern analogues technique for palaeoclimate reconstruction in arid and semi-arid regions. Boreas, 39: 145–153
Jiang W Y, Guo Z T, Sun X J, Wu H B, Chu G Q, Yuan B Y, Hatté C, Guiot J. 2006. Reconstruction of climate and vegetation changes of Lake Bayanchagan (Inner Mongolia): Holocene variability of the East Asian monsoon. Quat Res, 65: 411–420
Jiang W Y, Yang S L, Yang X X, Gu N. 2016. Negative impacts of afforestation and economic forestry on the Chinese Loess Plateau and proposed solutions. Quat Int, 399: 165–173
Jiang W Y, Yang X X, Cheng Y F. 2014. Spatial patterns of vegetation and climate on the Chinese Loess Plateau since the Last Glacial Maximum. Quat Int, 334-335: 52–60
Jin H, Dong G, Su Z, Sun L. 2001. Reconstruction of the spatial patterns of desert/loess boundary belt in North China during the Holocene. Chin Sci Bull, 46: 969–974
Johnson R G, McClure B T. 1976. A model for northern hemisphere continental ice sheet variation. Quat Res, 6: 325–353
Kennett D J, Kennett J P, West A, Mercer C, Hee S S Q, Bement L, Bunch T E, Sellers M, Wolbach W S. 2009. Nanodiamonds in the Younger Dryas boundary sediment layer. Science, 323: 94
Lambeck K, Rouby H, Purcell A, Sun Y, Sambridge M. 2014. Sea level and global ice volumes from the Last Glacial Maximum to the Holocene. Proc Natl Acad Sci USA, 111: 15296–15303
Levitus S, Antonov J I, Boyer T P, Stephens C. 2000. Warming of the world ocean. Science, 287: 2225–2229
Li J, Wu Z, Jiang Z, He J. 2010. Can global warming strengthen the East Asian summer monsoon? J Clim, 23: 6696–6705
Li S, Sun W, Li X Z, Zhang B. 1995. Sedimentary characteristics and environmental evolution of Otindag sandy land in Holocene (in Chinese with English abstract). J Desert Res, 15: 323–331
Liu J, Chen J, Zhang X, Li Y, Rao Z, Chen F. 2015. Holocene East Asian summer monsoon records in northern China and their inconsistency with Chinese stalagmite δ^{18}O records. Earth-Sci Rev, 148: 194–208
Liu X M, Rolph T, Bloemendal J, Shaw J, Liu T S. 1995. Quantitative estimates of palaeoprecipitation at Xifeng, in the loess plateau of China. Palaeogeogr Palaeoclimatol Palaeoecol, 113: 243–248
Liu Y S C, Utescher T, Zhou Z, Sun B. 2011. The evolution of Miocene climates in North China: Preliminary results of quantitative reconstructions from plant fossil records. Palaeogeogr Palaeoclimatol Palaeoecol, 304: 308–317
Liu Z, Otto-Bliesner B L, He F, Brady E C, Tomas R, Clark P U, Carlson A E, Lynch-Stieglitz J, Curry W, Brook E, Erickson D, Jacob R, Kutzbach J, Cheng J. 2009. Transient simulation of last deglaciation with a new mechanism for Bølling-Allerød warming. Science, 325: 310–314
Lu H Y, Han J M, Wu N Q, Guo Z T. 1994. Magnetic susceptibility of the modern soils in China and paleoclimatic significance (in Chinese). Sci China Ser B, 24: 1290–1297
Lu H Y, Wu N Q, Liu K B, Jiang H, Liu T S. 2007. Phytoliths as quantitative indicators for the reconstruction of past environmental conditions in China II: Palaeoenvironmental reconstruction in the Loess Plateau. Quat Sci Rev, 26: 759–772
Lu H Y, Yi S W, Xu Z W, Zhou Y L, Zeng L, Zhu F Y, Feng H, Dong L N, Zhuo H X, Yu K F, Mason J, Wang X Y, Chen Y Y, Lu Q, Wu B, Dong Z B, Qu J J, Wang X M, Guo Z T. 2013b. Chinese deserts and sand fields in Last Glacial Maximum and Holocene Optimum. Chin Sci Bull, 58: 2775–2783
Lu H, Yi S, Liu Z, Mason J A, Jiang D, Cheng J, Stevens T, Xu Z, Zhang E, Jin L, Zhang Z, Guo Z, Wang Y, Otto-Bliesner B. 2013a. Variation of East Asian monsoon precipitation during the past 21 k.y. and potential CO_2 forcing. Geology, 41: 1023–1026
Lüthi D, Le Floch M, Bereiter B, Blunier T, Barnola J M, Siegenthaler U, Raynaud D, Jouzel J, Fischer H, Kawamura K, Stocker T F. 2008. High-resolution carbon dioxide concentration record 650000–800000 years before present. Nature, 453: 379–382
Ma Z B, Cheng H, Tan M, Edwards R L, Li H C, You C F, Duan W H, Wang X, Kelly M J. 2012. Timing and structure of the Younger Dryas event in northern China. Quat Sci Rev, 41: 83–93
Maher B A, Thompson R, Zhou L P. 1994. Spatial and temporal reconstructions of changes in the Asian palaeomonsoon: A new mineral magnetic approach. Earth Planet Sci Lett, 125: 461–471
Mason J A, Lu H, Zhou Y, Miao X, Swinehart J B, Liu Z, Goble R J, Yi S. 2009. Dune mobility and aridity at the desert margin of northern China at a time of peak monsoon strength. Geology, 37: 947–950
Nakagawa T, Tarasov P E, Kitagawa H, Yasuda Y, Gotanda K. 2006. Seasonally specific responses of the East Asian monsoon to deglacial climate changes. Geology, 34: 521–524
Peterse F, Martínez-García A, Zhou B, Beets C J, Prins M A, Zheng H,

Eglinton T I. 2014. Molecular records of continental air temperature and monsoon precipitation variability in East Asia spanning the past 130000 years. Quat Sci Rev, 83: 76–82
Porter S C, An Z S. 1995. Correlation between climate events in the North Atlantic and China during the last glaciation. Nature, 375: 305–308
Qian W H, Lin X, Zhu Y F, Xu Y, Fu J L. 2007. Climatic regime shift and decadal anomalous events in China. Clim Change, 84: 167–189
Quade J, Broecker W S. 2009. Dryland hydrology in a warmer world: Lessons from the Last Glacial period. Eur Phys J Spec Top, 176: 21–36
Rehfeld K, Laepple T. 2016. Warmer and wetter or warmer and dryer? Observed versus simulated covariability of Holocene temperature and rainfall in Asia. Earth Planet Sci Lett, 436: 1–9
Rooth C. 1982. Hydrology and ocean circulation. Prog Oceanography, 11: 131–149
Severinghaus J P, Brook E G. 1999. Abrupt climate change at the end of the last glacial period inferred from trapped air in polar ice. Science, 286: 930–934
Shen J. 2013. Spatiotemporal variations of Chinese lakes and their driving mechanisms since the Last Glacial Maximum: A review and synthesis of lacustrine sediment archives. Chin Sci Bull, 58: 17–31
Siegert M J, Dowdeswell J A, Melles M. 1999. Late weichselian glaciation of the Russian high arctic. Quat Res, 52: 273–285
Snyder C W. 2016. Evolution of global temperature over the past two million years. Nature, 538: 226–228
Stebich M, Mingram J, Han J T, Liu J Q. 2009. Late Pleistocene spread of (cool-)temperate forests in Northeast China and climate changes synchronous with the North Atlantic region. Glob Planet Change, 65: 56–70
St-Onge G, Stoner J S, Hillaire-Marcel C. 2003. Holocene paleomagnetic records from the St. Lawrence Estuary, eastern Canada: Centennial- to millennial-scale geomagnetic modulation of cosmogenic isotopes. Earth Planet Sci Lett, 209: 113–130
Sun J M. 2000. Origin of eolian sand mobilization during the past 2300 years in the Mu Us Desert, China. Quat Res, 53: 78–88
Sun J M, Ding Z L, Liu T S. 1998. Desert distributions during the glacial maximum and climatic optimum: Example of China. Episodes, 21: 28–31
Sun J M, Zhang Z Q, Zhang L Y. 2009. New evidence on the age of the Taklimakan Desert. Geology, 37: 159–162
Svendsen J I, Alexanderson H, Astakhov V I, Demidov I, Dowdeswell J A, Funder S, Gataullin V, Henriksen M, Hjort C, Houmark-Nielsen M, Hubberten H W, Ingólfsson Ó, Jakobsson M, Kjær K H, Larsen E, Lokrantz H, Lunkka J P, Lysså A, Mangerud J, Matioushkov A, Murray A, Möller P, Niessen F, Nikolskaya O, Polyak L, Saarnisto M, Siegert C, Siegert M J, Spielhagen R F, Stein R. 2004. Late Quaternary ice sheet history of northern Eurasia. Quat Sci Rev, 23: 1229–1271
Svensson A, Andersen K K, Bigler M, Clausen H B, Dahl-Jensen D, Davies S M, Johnsen S J, Muscheler R, Parrenin F, Rasmussen S O, Röthlisberger R, Seierstad I, Steffensen J P, Vinther B M. 2008. A 60000 year Greenland stratigraphic ice core chronology. Clim Past, 4: 47–57
Tan M, Liu T S, Hou J Z, Qin X G, Zhang H C, Li T Y. 2003. Cyclic rapid warming on centennial-scale revealed by a 2650-year stalagmite record of warm season temperature. Geophys Res Lett, 30: 1617
Tang X, Chen B D, Liang P, Qian W H. 2010. Definition and features of the north edge of the East Asian summer monsoon. Acta Meteorol Sin, 24: 43–49
Tao S Y, Chen L X. 1987. A review of recent research on the East Asian Summer Monsoon in China. In: Chang C P, Krishnamurti T N, eds. Monsoon Meteorology. Oxford: Oxford University Press. 60–92
Turner T E, Swindles G T, Charman D J, Langdon P G, Morris P J, Booth R K, Parry L E, Nichols J E. 2016. Solar cycles or random processes? Evaluating solar variability in Holocene climate records. Sci Rep, 6: 23961
Wang B, Clemens S C, Liu P. 2003. Contrasting the Indian and East Asian monsoons: Implications on geologic timescales. Mar Geol, 201: 5–21
Wang H. 2001. The weakening of the Asian monsoon circulation after the end of 1970's. Adv Atmos Sci, 18: 376–386
Wang N A, Li Z, Li Y, Cheng H, Huang R. 2012. Younger Dryas event recorded by the mirabilite deposition in Huahai lake, Hexi Corridor, NW China. Quat Int, 250: 93–99
Wang P X, Bian Y H, Li B H, Huang C Y. 1996. The Younger Dryas in the West Pacific marginal seas (in Chinese). Sci China Ser-D Earth Sci, 39: 522–532
Wang P X. 2009. Global monsoon in a geological perspective. Chin Sci Bull, 54: 1113–1136
Wang S M, Ji L, Yang X D, Xue B, Ma Y, Hu S Y. 1994. The record of Younger Dryas event in lake sediments from Jalai Nur, Inner Mongolia (in Chinese). Chin Sci Bull, 39: 831–835
Wang Y J, Cheng H, Edwards R L, He Y Q, Kong X G, An Z S, Wu J Y, Kelly M J, Dykoski C A, Li X D. 2005. The Holocene Asian monsoon: Links to solar changes and North Atlantic climate. Science, 308: 854–857
Wang Y J, Cheng H, Edwards R L, Kong X G, Shao X H, Chen S T, Wu J Y, Jiang X Y, Wang X F, An Z S. 2008. Millennial- and orbital-scale changes in the East Asian monsoon over the past 224000 years. Nature, 451: 1090–1093
Wang Y, Amundson R, Trumbore S. 1996. Radiocarbon dating of soil organic matter. Quat Res, 45: 282–288
Wang Y, Liu X, Herzschuh U. 2010. Asynchronous evolution of the Indian and East Asian Summer Monsoon indicated by Holocene moisture patterns in monsoonal central Asia. Earth-Sci Rev, 103: 135–153
Webster P J, Magaña V O, Palmer T N, Shukla J, Tomas R A, Yanai M, Yasunari T. 1998. Monsoons: Processes, predictability, and the prospects for prediction. J Geophys Res, 103: 14451–14510
Wen R L, Xiao J L, Chang Z G, Zhai D Y, Xu Q H, Li Y C, Itoh S, Lomtatidze Z. 2010a. Holocene climate changes in the mid-high-latitude-monsoon margin reflected by the pollen record from Hulun Lake, northeastern Inner Mongolia. Quat Res, 73: 293–303
Wen R L, Xiao J L, Chang Z G, Zhai D Y, Xu Q H, Li Y C, Itoh S. 2010b. Holocene precipitation and temperature variations in the East Asian monsoonal margin from pollen data from Hulun Lake in northeastern Inner Mongolia, China. Boreas, 39: 262–272
Wen R L, Xiao J L, Fan J W, Zhang S R, Yamagata H. 2017. Pollen evidence for a mid-Holocene East Asian summer monsoon maximum in northern China. Quat Sci Rev, 176: 29–35
Wu J, Liu Q, Wang L, Chu G Q, Liu J Q. 2016. Vegetation and climate change during the last deglaciation in the Great Khingan Mountain, Northeastern China. Plos One, 11: e0146261
Wu X H, An Z S, Wang S M, Liu X D, Li X Q, Zhou W J, Liu J F, Lu J J, Porter S C, Kutzbach J E. 1994. The temporal and spatial variation of East Asian Summer Monsoon in Holocene optimum in China (in Chinese with English abstract). Quat Sci, 14: 24–37
Xiao J L, Chang Z G, Wen R L, Zhai D Y, Itoh S, Lomtatidze Z. 2009. Holocene weak monsoon intervals indicated by low lake levels at Hulun Lake in the monsoonal margin region of northeastern Inner Mongolia, China. Holocene, 19: 899–908
Xiao J L, Si B, Zhai D Y, Itoh S, Lomtatidze Z. 2008. Hydrology of Dali Lake in central-eastern Inner Mongolia and Holocene East Asian monsoon variability. J Paleolimnol, 40: 519–528
Xiao J L, Xu Q H, Nakamura T, Yang X L, Liang W D, Inouchi Y. 2004. Holocene vegetation variation in the Daihai Lake region of north-central China: A direct indication of the Asian monsoon climatic history. Quat Sci Rev, 23: 1669–1679
Xu D K, Lu H Y, Chu G Q, Wu N Q, Shen C M, Wang C, Mao L M. 2014. 500-year climate cycles stacking of recent centennial warming documented in an East Asian pollen record. Sci Rep, 4: 3611
Xu Q H, Xiao J L, Li Y C, Tian F, Nakagawa T. 2010. Pollen-based quantitative reconstruction of Holocene climate changes in the Daihai Lake area, Inner Mongolia, China. J Clim, 23: 2856–2868
Yang F, Lau K M. 2004. Trend and variability of China precipitation in spring and summer: Linkage to sea-surface temperatures. Int J Climatol, 24: 1625–1644
Yang L R, Yue L P. 2011. The environmental transformation from late last

glacial to Holocene of Otindag sandyland (in Chinese with English abstract). J Earth Environ, 2: 301–306
Yang S L, Ding Z L. 2008. Advance-retreat history of the East-Asian summer monsoon rainfall belt over northern China during the last two glacial-interglacial cycles. Earth Planet Sci Lett, 274: 499–510
Yang S L, Ding Z L. 2014. A 249 kyr stack of eight loess grain size records from northern China documenting millennial-scale climate variability. Geochem Geophys Geosyst, 15: 798–814
Yang S L, Ding Z L, Feng S H, Jiang W Y, Huang X F, Guo L C. 2018. A strengthened East Asian Summer Monsoon during Pliocene warmth: Evidence from 'red clay' sediments at Pianguan, northern China. J Asian Earth Sci, 155: 124–133
Yang S L, Ding Z L, Li Y Y, Wang X, Jiang W Y, Huang X F. 2015. Warming-induced northwestward migration of the East Asian monsoon rain belt from the Last Glacial Maximum to the mid-Holocene. Proc Natl Acad Sci USA, 112: 13178–13183
Yang X X, Jiang W Y, Yang S L, Kong Z C, Luo Y L. 2015. Vegetation and climate changes in the western Chinese Loess Plateau since the Last Glacial Maximum. Quat Int, 372: 58–65
Zhou W J, Yu X F, Jull A J T, Burr G, Xiao J Y, Lu X F, Xian F. 2004. High-resolution evidence from southern China of an early Holocene optimum and a mid-Holocene dry event during the past 18000 years. Quat Res, 62: 39–48
Zhou X, Sun L G, Zhan T, Huang W, Zhou X Y, Hao Q Z, Wang Y H, He X Q, Zhao C, Zhang J, Qiao Y S, Ge J Y, Yan P, Yan Q, Shao D, Chu Z D, Yang W Q, Smol J P. 2016. Time-transgressive onset of the Holocene Optimum in the East Asian monsoon region. Earth Planet Sci Lett, 456: 39–46
Zhu Z D. 1998. Concept, cause and control of desertification in China (in Chinese with English abstract). Quat Sci, 18: 145–155

(Responsible editor: Xiaoqiang LI)